THE JOURNAL OF PHYSICAL CHEMISTRY C

Article

pubs.acs.org/JPCC

Search for a Metallic Dangling-Bond Wire on *n*-Doped H-Passivated Semiconductor Surfaces

Mads Engelund,*[,†] Nick Papior,[‡,§] Pedro Brandimarte,[†] Thomas Frederiksen,[∥,⊥] Aran Garcia-Lekue,[∥,⊥] and Daniel Sánchez-Portal[†,∥]

[†]Centro de Física de Materiales (CFM) CSIC-UPV/EHU, Paseo Manuel de Lardizabal 5, E-20018 Donostia-San Sebastián, Spain

[‡]DTU Nanotech, Ørsted Plads, building 345E, DK-2800 Kgs. Lyngby, Denmark

[§]Center for Nanostructured Graphene, CNG, DK-2800 Kgs. Lyngby, Denmark

[∥]Donostia International Physics Center, DIPC, Paseo Manuel de Lardizabal 4, E-20018 Donostia-San Sebastián, Spain

[⊥]IKERBASQUE, Basque Foundation for Science, E-48013 Bilbao, Spain

ABSTRACT: We have theoretically investigated the electronic properties of neutral and *n*-doped dangling bond (DB) quasi-one-dimensional structures (lines) in the Si(001):H and Ge(001):H substrates with the aim of identifying atomic-scale interconnects exhibiting metallic conduction for use in on-surface circuitry. Whether neutral or doped, DB lines are prone to suffer geometrical distortions or have magnetic ground states that render them semiconducting. However, from our study we have identified one exception—a dimer row fully stripped of hydrogen passivation. Such a DB-dimer line shows an electronic band structure which is remarkably insensitive to the doping level, and thus, it is possible to manipulate the position of the Fermi level, moving it away from the gap. Transport calculations demonstrate that the metallic conduction in the DB-dimer line can survive thermally induced disorder but is more sensitive to imperfect patterning. In conclusion, the DB-dimer line shows remarkable stability to doping and could serve as a one-dimensional metallic conductor on *n*-doped samples.

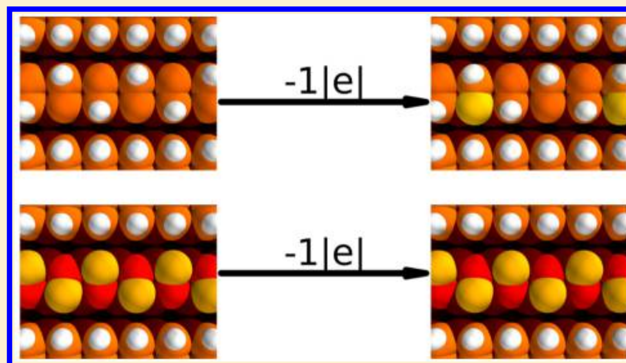

■ INTRODUCTION

The dream of fabricating structures with atomic precision has become a reality in certain semiconductor substrates. Local hydrogen desorption, induced with the aid of a scanning tunnelling microscope (STM) tip, on the hydrogen-passivated (1 × 2)-reconstruction of the Si(001) and Ge(001) substrates [hereafter Si/Ge(001):H] can be used to reproducibly and rapidly create dangling-bond (DB) arrays defined with atomic precision.[1−4] This is a powerful method that allows one to directly pattern planar electronic devices and circuitry made out of DBs[5−10] and to create templates for anchoring molecular networks[11−15] or for selective dopant incorporation.[16−19] DB arrays have a very rich and complex behavior, exhibiting several metastable charge- and spin-states,[4,20−27] as well as small polaron and soliton formation.[28,29] While this complexity makes the study of these systems attractive from a fundamental point of view, it might hinder their use for technological applications. In particular, it would be desirable to have a practical scheme to fabricate simple conductive wiring for interconnecting complex functional units of atomic dimensions (e.g., atomic and molecular logic gates[30−33]) deposited or patterned on semiconductor substrates.[34]

There have been several theoretical proposals of logic gates constructed with DBs on Si/Ge(001):H surfaces.[10,33] A recent joint experimental and theoretical work has demonstrated the operation of one such device.[35] In that experiment, however, the DB gate was addressed using STM tips, which does not represent a scalable technology. For this to be realized in practice, it would be highly desirable that atomic-scale wiring could be created directly on the surface via a simple procedure. Given the existing techniques, the possibility to fabricate atomic-scale metallic connectors made out of DBs on Si/Ge(001):H would be highly attractive. This, together with the ability to fabricate logic elements using DBs as building blocks, would allow creating a full circuit in a single processing step with atomic-scale precision. Unfortunately, quasi-one-dimensional (1D) structures formed by DBs are prone to suffer from instabilities that open gaps in the electronic band structure, making them less than ideal candidates for atomic-scale interconnects.[1,20,36,37] In such cases, electron transport can still occur through diffusion of polarons,[28] but transport in this regime is typically less efficient.

Half-filled electron bands in 1D structures are particularly prone to suffer distortions that destroy the metallicity of the

Received: May 5, 2016
Revised: August 5, 2016
Published: August 23, 2016

ACS Publications © 2016 American Chemical Society

DOI: 10.1021/acs.jpcc.6b04540
J. Phys. Chem. C 2016, 120, 20303−20309

system.[38−41] A possible strategy to enforce a metallic character of the DB lines could be to dope the system with holes or electrons, moving the systems away from the half-filled condition. The idea is that this would move the Fermi energy away from the band gap provided that the band structure remains more or less constant.

The concept of moving the Fermi level away from the band gap by doping the system is particularly attractive due to its simplicity. However, it is in general far from certain that the geometric and electronic structure of the DB lines remains unchanged under different electron fillings. The purpose of the present theoretical study is to clarify this issue for several key structures of DB lines on both Si(001):H and Ge(001):H substrates. Few studies have so far addressed this interplay between doping and stability and then only for one type of DB line.[23,28] Yet doping is both an important experimental parameter and largely unavoidable, even in supposedly pristine substrates.[42]

We limit our investigation to *n*-type doping because unoccupied DB-derived electronic features tend to lie in the bandgap, whereas the occupied ones are either resonant with, or close to, the bulk valence bands of both Si[4,36] and Ge.[1] Therefore, we judge *p*-type doping as less likely to yield functional wires since DB-derived bands would only be weakly localized to the DB lines.

We have investigated four basic DB lines. Three of these lines follow the basic dimer rows of the Si/Ge(001):H surfaces, and one is perpendicular to these rows (see Figure 1). The investigated structures are, (A) the removal of all H atoms from one side of the dimers along one row ("Si/Ge-straight"), (B) the removal of H on alternating sides of the dimers along one row ("Si/Ge-zigzag"), (C) the perpendicular structure formed by the removal of both H atoms from one dimer on each dimer row ("Si/Ge-across"), and finally (D) the complete hydrogen removal from one dimer row ("Si/Ge-dimer").

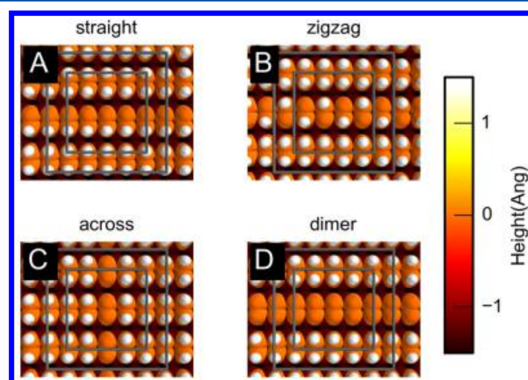

Figure 1. Top view of the four basic DB line structures investigated in this paper. The structures are idealized; i.e., they correspond to the situation in which all Si/Ge atoms along the DB lines are equivalent. Small spheres represent hydrogen atoms, while large ones represent Si or Ge atoms. Atoms are colored according to their height on the surface, and the surface unit cells considered in this study ((2 × 4) or (3 × 6)) are shown as gray squares.

COMPUTATIONAL METHODS

The DB lines have been studied by spin-polarized density functional theory (DFT) using the SIESTA code.[43] The slabs used in the calculations contain 8 Si/Ge layers, including the reconstructed Si/Ge surface layer. A (2 × 4) surface supercell was used. Atoms in the lower layer of the slab, which follow a bulk-like arrangement, are passivated with hydrogen. Relaxations were performed with a force tolerance of 0.02 eV/Å, fixing the lower 4 Si/Ge layers as well as the hydrogen-passivated layer at the bottom of the slab. The configurations were initialized using the Si/Ge(001):H positions, with a fully polarized spin structure, and one DB site was raised either 0.01 or 0.4 Å. Those configurations which relaxed to a spin-polarized final state were reinitialized to ensure that both ferromagnetic and antiferromagnetic ordering was attempted.

We used the generalized gradient approximation (GGA) to describe exchange and correlation,[44] a mesh cutoff of 200 Ry for real-space integrations, a double-ζ plus polarization (DZP) basis set generated with an energy shift[43] of 150 meV, and a (6 × 3) *k*-point grid, with the highest sampling along the direction of the 1D DB line. Local-density approximation (LDA) calculations were performed to test the stability of our conclusions with respect to the exchange-correlation functional used. For the Si substrate GGA functional calculations with a larger (3 × 6) supercell and 10 layers (8 of them relaxed) were performed for all lines to verify that our conclusions are robust against the number of layers present and relaxed in the slab, the distance between the DB lines, and the length of the DB-line portion explicitly considered. The level of approximation was chosen to reproduce structural deformations as well as qualitative features of the electronic structure.

RESULTS AND DISCUSSION

The main question to solve is whether it is possible to achieve a conducting DB wire by doping or if the excess carriers will tend to localize, thereby creating a new distortion pattern.

To simulate the *n*-doping of the DB lines, we doped the system with extra electrons and compensated their charge by adding a homogeneous positive charge background so the system remained globally neutral. We decided to use integer number of electrons in our calculations since small fractional charging of the unit cell would artificially suppress the formation of localized charge distortions. On the other hand, this means that we limit ourselves to simulating relatively large doping levels. These calculations allow us to determine if excess electrons tend to enter delocalized states of the extended 1D line or cause polaron formation.

Our calculations model uniform doping, i.e., a situation where dopants do not tend to segregate to the surface, and thus, their number close to the surface might be considered as negligible. If special care is taken to avoid surface depletion of dopants under preparation, the specifics of dopant type and placement could become important to determine the properties of DB lines under doping.[23,45]

Since few qualitative differences were seen between Si(001):H and Ge(001):H, we show only the Si results in the figures and mention the differences between both substrates in the text.

As a starting point we naturally investigated the properties of the undoped DB lines (see Figure 2, left column). The first thing to note is that all the DB lines exhibit band gaps with no states at the Fermi level in the absence of doping (hereafter we refer to this undoped situation as "neutral"). These gaps, however, have two types of origins: (*i*) a geometric distortion combined with charge transfer between DBs occupying inequivalent positions and (*ii*) local spin polarization which opens a gap in the spin-polarized band structure. These two effects compete since charge reorganization tends to create

DOI: 10.1021/acs.jpcc.6b04540
J. Phys. Chem. C 2016, 120, 20303−20309

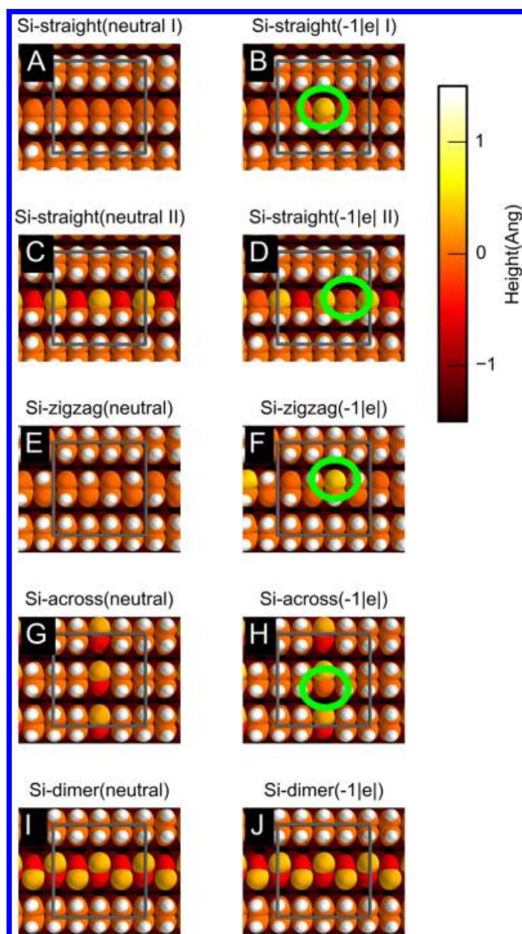

Figure 2. Relaxed structures of different DB lines in Si(001):H. Neutral structures and those with one extra electron in the simulation cell are compared. Two structures are shown for the Si-straight line as explained in the text: neutral I corresponds to the antiferromagnetic ordered ground state, while neutral II shows the structurally distorted configuration lying only 5 meV per DB higher in energy. Atoms are colored according their height. The green rings in panels B, D, F, and H highlight the DB site which undergoes a geometric distortion upon doping.

doubly and unoccupied DB sites, while spin polarization tends to create singly occupied DB sites. From a structural point of view, DB sites come in roughly three groups, raised position (doubly occupied), neutral position (singly occupied), and lowered position (unoccupied).

In agreement with earlier studies,[1,20] we find that the most stable solution for Si/Ge-across and Si/Ge-dimer lines corresponds to a strong geometric distortion, while the Si/Ge-zigzag structures undergo a magnetic distortion (in which all DB sites have the same population and, thus, the same height over the substrate). For the Si/Ge-straight line both magnetically distorted states and unpolarized states with geometric distortion could be stabilized. For the Ge-straight line we calculate that the geometrically distorted state is more stable by 100 meV per DB than a magnetically distorted state with antiferromagnetic ordering, while the corresponding value for the Si-straight line is less than 5 meV per DB. In the latter case, this energy difference is too small to confidently assign either of these solutions as the ground state of the system due to different limitations in our model, such as the spin contamination of unrestricted DFT calculations.[46−48]

In contrast, the two lines made up of unpassivated dimers, the Si/Ge-across and Si/Ge-dimer lines, are less sensitive to initial conditions and invariably relax to a geometrically distorted configuration where each dimer contains both doubly and unoccupied sites. It is, however, possible to stabilize different patterns due to the relative orientations of the dimers in the lines—something we will discuss in detail later. In general, different structures on Ge(001):H tend to be better separated in energy than those on Si(001):H. For example, the Ge-straight DB line is more stable by 140 meV per DB site than the Ge-zigzag DB line, while the corresponding number for Si(001):H is only 50 meV per DB.

Moving on to the *n*-doped results (see the right column of Figure 2), upon charging with one electron the Si/Ge-straight, Si/Ge-zigzag, and Si/Ge-across lines show a strong geometric distortion for at least one DB site (compare Figures 2A,C,E,G to Figures 2B,D,F,H), while the Si/Ge-dimer lines do not exhibit such distortion (no visible change from Figure 2I to Figure 2J).

The Si/Ge-zigzag DB line can be used as an example of a structure that can undergo geometric distortions. Figure 3 shows that, as charge is added, local geometrical distortions are coupled to the localization of the extra carriers at specific sites. The Si/Ge-zigzag DB line gains one electron, and one DB site becomes fully occupied, removing the spin polarization at that site and moving the corresponding atom to a higher position

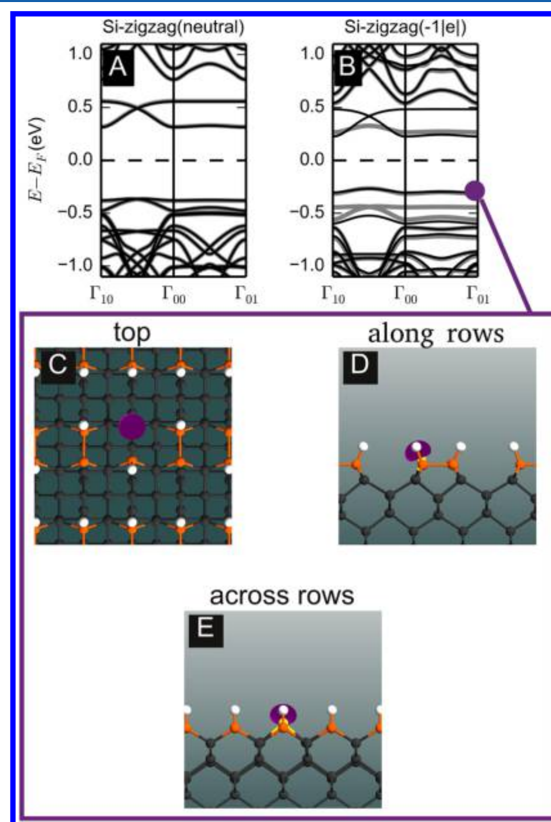

Figure 3. Band structures of the Si-zigzag 1D line: (A) neutral and (B) doped with one extra electron per cell. The band structure path goes from Γ-point to Γ-point, first along the DB line ($\Gamma_{10} - \Gamma_{00}$), then along the transverse direction ($\Gamma_{00} - \Gamma_{01}$). Majority (minority) bands are shown as thin black (thick gray) lines. (C−E) Isosurface plots (0.05 eÅ^{-3} isovalue) of the density associated with the spin-degenerate band marked in panel B.

DOI: 10.1021/acs.jpcc.6b04540
J. Phys. Chem. C 2016, 120, 20303−20309

(as highlighted in Figure 2F). As a consequence, the Fermi level lies within the new gap, and the band structure remains insulating. As previously observed by Bowler and Fisher[28] for the Si-straight DB line, the extra electron becomes self-trapped and forms a small polaron. We note that this is only one possible configuration of the charged Si/Ge-zigzag and Si/Ge-straight lines since the competition between charge and spin-polarization produces a large number of metastable states. However, it is clear that the neutral ground state is not stable under charging.

In striking contrast with the rest of the DB lines, the simple picture of doping holds for the Si/Ge-dimer system: as seen in Figure 4, when electrons are added to the cell, both the geometric and electronic structures remain stable. The changes of the geometric structure are small since the additional charge distributes homogeneously along the DB line and, as a consequence, the changes of the band structure correspond mostly to a rigid shift of the Fermi level. In general, we observe that the basic features of the electronic band structure persist until the Fermi level reaches the conduction band edge, at which point any additional electrons will occupy the conduction band (see Figure 4F). If we assume that this stability occurs also at the intermediate doping values between calculations, we conclude that the structure should be stable and metallic at any level of excess electrons near the surface. However, we should always be aware that the presence of excess electrons at the surface is not guaranteed even on nominally n-doped substrates.[42] These results are consistent with the experimental scanning tunnelling spectroscopy data by Naydenov and Boland,[36] who demonstrated that the Si-straight structures exhibit no states at the Fermi level while the Si-dimer does.

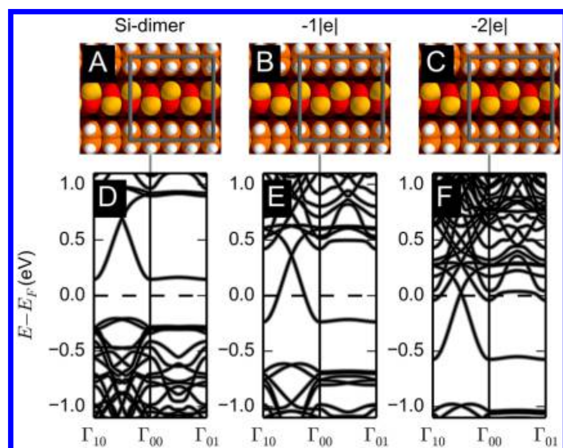

Figure 4. (A−C) Relaxed geometries and (D−F) electronic band structures of the Si-dimer DB line in the neutral state and charged with one and two extra electrons in the (2 × 4) supercell (corresponding to 1/8 and 1/4 electrons per DB site, respectively). These spin-degenerate band structures follow the same path as those in Figure 3.

In general, very similar results are found for the two substrates. The important edge case was the Si/Ge-straight DB lines where we found two possible ground-state structures for the Si-straight line. However, by explicitly initializing the charged calculations for both substrates from both possible ground states (nonmagnetic and buckled, spin-polarized and flat), in all cases we observe stabilization of a self-trapped polaron when adding extra electrons to the system. The Ge-straight DB line is also the only structure where we observed a qualitative difference when using different exchange-correlation functionals. In contrast to the GGA case, our LDA results predict the buckled Ge-straight DB line to be stable with respect to charging. Otherwise, our doping results are robust with respect to both substrate and functional.

After our investigation, the Si/Ge-dimer DB line clearly stands out. When doped with electrons it retains its geometric and electronic structure in marked contrast to the three other DB lines investigated. Having identified the n-doped Si/Ge-dimer DB lines as possible candidates for conducting wires, we now proceed to investigate their transport properties and, in particular, how these properties are influenced by simple defects which are likely to be present in such wires. This is a crucial piece of information for the applicability of these structures as interconnects in atomic-scale circuits.

To examine possible disruptions of the Si/Ge-dimer wire, we have investigated two types of defects, a "hydrogen defect" and a "phase-shift" defect (see Figure 5). The hydrogen defect is simply the repassivation of a single DB site in the structure by a hydrogen atom—a type of defect which could occur due to imperfect hydrogen removal. The phase-shift defect consists of two dimers which are slanted in the *same* direction, while the remaining dimers are slanted following the normal alternating pattern. The phase-shift defect is effectively the boundary point between two domains of the DB-dimer line with oppositely alternating patterns. From entropic considerations, a sufficiently long DB-dimer line will have multiple alternating domains and thereby phase shift defects—the boundary between the domains. We have estimated the energy cost of creating a phase-shift defect to be ∼100 meV for both Si and Ge by comparing the total energies of an ideal DB-dimer line and a DB-dimer line containing a phase-shift defect in a (2 × 9) supercell. This energetic cost means that we can expect approximately one phase-shift defect in every 50 dimers in thermal equilibrium at room temperature. At liquid nitrogen temperatures the occurrence of these defects from thermal fluctuations should be negligible, but we assume that they could be easily created during the surface patterning process—on

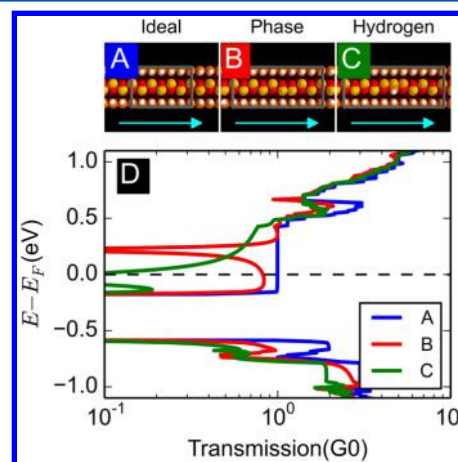

Figure 5. (A−C) Relaxed structures and (D) transmission spectrum relative to the Fermi level for a DB-dimer line with different types of defects on Si(001):H. Transmission curves are shown for a (A) an ideal Si-dimer wire, (B) a phase-shift defect, and (C) a hydrogen defect with a doping corresponding to 1/8 electrons per DB site. None of these structures exhibits spin polarization at this doping level, so both spin channels have the same transmission.

DOI: 10.1021/acs.jpcc.6b04540
J. Phys. Chem. C 2016, 120, 20303−20309

purpose or inadvertently—e.g., if domains of different alternation are created separately and then connected.

Electron transport across these defects was investigated using the TranSIESTA code.[49] These calculations were performed using open-boundary conditions and (2 × 6), (2 × 9), and (2 × 10) simulation cells for the ideal wire, phase-shift, and hydrogen defects, respectively. These supercells include the central scattering region and (2 × 2) blocks in either end, corresponding to the electrodes, and a consistent level of doping per dimer row was used in the electrode and full calculations. For transmission calculations a (7 × 1) *k*-point sampling in the directions transverse to the transport direction was used.

Figure 5 shows the transmission curves for each type of defect and a doping level corresponding to 1/8 electrons per DB (or 1/4 electrons per unsaturated DB-dimer) in Si(001):H. As earlier, the results are very similar in the case of Ge DB-dimer lines. For this level of doping, a single phase-shift defect reduces the transmission at the Fermi level from 1 to 0.8 (0.9) for Si (Ge). In other words, ∼10% of the transmission survives after propagation through 10 (21) phase-shift defects. At room temperature and assuming that this is the only type of defect present, this would correspond to wires containing more than ∼500 (1000) DB-dimers. The geometric and electronic structure of the phase-shift defect is insensitive to the doping level—similarly to the Si/Ge-dimer wire itself. Due to this and the relatively constant transmission curve our estimate should hold also at lower doping levels. To explore the stability of the structure under bias, we have performed a relaxation with a 0.2 V voltage drop across the defect structure. We find that essentially no further relaxation takes place and that the transmission is relatively constant in the bias window. All in all, the presence of the phase-shift defect does not seem to greatly diminish the metallic character of the wire.

The hydrogen defect is more complex since the structure and spin-polarization change with the doping level. The DB site next to the hydrogen defect (within the same DB-dimer) can be neutral or negatively charged depending on the doping level and the substrate. At the (high) doping level presented in Figure 5, the hydrogen defect is negatively charged (and nonmagnetic), and the presence of the defect almost completely turns off the transmission at the Fermi level. Lowering the doping level results in a neutral defect on both substrates; i.e., the DB next to the hydrogen atom is only occupied by an unpaired electron, and as a consequence, it is spin-polarized. The neutral hydrogen defect results in different scattering for carriers with different spin orientations. Despite this complex behavior though, the conclusion is simple—the uncontrolled inclusion of a single hydrogen defect is likely to break the intended functionality.

■ CONCLUSION

As we have seen, surface DB structures are highly complex due to the delicate interplay between their geometric, electronic, and magnetic properties. Electrons tend to localize at DB sites generating both geometrical distortions and ordered magnetic arrangements that usually translate onto the opening of gaps at the Fermi level in the electronic band structure. This makes it difficult to achieve a simple metallic wire made exclusively of surface DBs. Although this does not diminish the potential of DB nanostructures to be used for other atomic-scale electronic devices which could harness the complexity, for example to fabricate logic gates or tunneling devices, this situation certainly limits their applicability as stable metallic interconnects.

However, we have found that stripping a full dimer row of hydrogen passivation is a promising route to achieve metallic interconnects on *n*-doped Si(001):H and Ge(001):H substrates at low temperatures. Our calculations predict that excess electrons do not localize along the DB-dimer lines and that the scattering from likely structural distortions would be relatively low. On the other hand, some impurities, such as repassivated DB sites, would need to be tightly controlled for the DB-dimer to retain conductivity. If structural impurities can be eliminated, using such interconnects would allow reaping the benefits of a single processing step when making on-surface circuits based on DB nanostructures.

From a practical point of view, DB arrays based on DB-dimers are also easier to fabricate since the ability to create DBs one-by-one has only been demonstrated on the silicon substrate,[5,50] while for germanium only dimer-by-dimer desorption has so far been demonstrated.[1] Achieving *n*-doping on Ge(001):H might be a practical problem since experiments have shown that an inversion layer occurs at the surface of *n*-doped samples.[42] However, if the construction of DB devices is combined with a technique to precisely incorporate phosphorus dopants in the subsurface region,[16,51] this problem might be overcome.

■ AUTHOR INFORMATION

Corresponding Author

*E-mail: mads.engelund@gmail.com. Phone: +34632702734.

Notes

The authors declare no competing financial interest.

■ ACKNOWLEDGMENTS

This work is funded by the FP7 FET-ICT “Planar Atomic and Molecular Scale devices” (PAMS) project (funded by the European Commission under contract No. 610446). ME, PB, TF, AGL, and DSP also acknowledge support from the Spanish Ministerio de Economía y Competitividad (MINECO) (Grant No. MAT2013-46593-C6-2-P) and the Basque Dep. de Educación and the UPV/EHU (Grant No. IT-756-13). MayaVi,[52] Matplotlib,[53] and Virtual NanoLab[54] were used in the preparation of figures. We thank Dr. Szymon Godlewski and Dr. Mathias Ljungberg for helpful discussions.

■ REFERENCES

(1) Kolmer, M.; Godlewski, S.; Kawai, H.; Such, B.; Krok, F.; Saeys, M.; Joachim, C.; Szymonski, M. Electronic properties of STM-constructed dangling-bond dimer lines on a Ge(001)-(2 × 1):H surface. *Phys. Rev. B: Condens. Matter Mater. Phys.* **2012**, *86*, 125307.

(2) Kolmer, M.; Godlewski, S.; Lis, J.; Such, B.; Kantorovich, L.; Szymonski, M. Construction of atomic-scale logic gates on a surface of hydrogen passivated germanium. *Microelectron. Eng.* **2013**, *109*, 262−265.

(3) Schofield, S. R.; Studer, P.; Hirjibehedin, C. F.; Curson, N. J.; Aeppli, G.; Bowler, D. R. Quantum engineering at the silicon surface using dangling bonds. *Nat. Commun.* **2013**, *4*, 1649.

(4) Engelund, M.; Zuzak, R.; Godlewski, S.; Kolmer, M.; Frederiksen, T.; García-Lekue, A.; Sánchez-Portal, D.; Szymonski, M. Tunneling spectroscopy of close-spaced dangling-bond pairs in Si(001):H. *Sci. Rep.* **2015**, *5*, 14496.

(5) Haider, M.; Pitters, J.; DiLabio, G.; Livadaru, L.; Mutus, J.; Wolkow, R. Controlled Coupling and Occupation of Silicon Atomic Quantum Dots at Room Temperature. *Phys. Rev. Lett.* **2009**, *102*, 046805.

DOI: 10.1021/acs.jpcc.6b04540
J. Phys. Chem. C 2016, 120, 20303−20309

(6) Godlewski, S.; Kolmer, M.; Kawai, H.; Such, B.; Zuzak, R.; Saeys, M.; de Mendoza, P.; Echavarren, A. M.; Joachim, C.; Szymonski, M. Contacting a Conjugated Molecule with a Surface Dangling Bond Dimer on a Hydrogenated Ge(001) Surface Allows Imaging of the Hidden Ground Electronic State. *ACS Nano* **2013**, *7*, 10105−10111.
(7) Pitters, J. L.; Dogel, I. A.; Wolkow, R. A. Charge Control of Surface Dangling Bonds Using Nanoscale Schottky Contacts. *ACS Nano* **2011**, *5*, 1984−1989.
(8) Livadaru, L.; Pitters, J.; Taucer, M.; Wolkow, R. A. Theory of nonequilibrium single-electron dynamics in STM imaging of dangling bonds on a hydrogenated silicon surface. *Phys. Rev. B: Condens. Matter Mater. Phys.* **2011**, *84*, 205416.
(9) Shaterzadeh-Yazdi, Z.; Livadaru, L.; Taucer, M.; Mutus, J.; Pitters, J.; Wolkow, R. A.; Sanders, B. C. Characterizing the rate and coherence of single-electron tunneling between two dangling bonds on the surface of silicon. *Phys. Rev. B: Condens. Matter Mater. Phys.* **2014**, *89*, 035315.
(10) Kawai, H.; Ample, F.; Wang, Q.; Yeo, Y. K.; Saeys, M.; Joachim, C. Dangling-bond logic gates on a Si(100)-(2 × 1)-H surface. *J. Phys.: Condens. Matter* **2012**, *24*, 095011.
(11) Lopinski, G. P.; Wayner, D. D. M.; Wolkow, R. A. Self-directed growth of molecular nanostructures on silicon. *Nature* **2000**, *406*, 48−51.
(12) Kruse, P.; Johnson, E. R.; DiLabio, G. A.; Wolkow, R. A. Patterning of Vinylferrocene on H-Si(100) via Self-Directed Growth of Molecular Lines and STM-Induced Decomposition. *Nano Lett.* **2002**, *2*, 807−810.
(13) Tong, X.; Dilabio, G. A.; Wolkow, R. A. A self-directed growth process for creating covalently bonded molecular assemblies on the H-Si(100)-3 × 1 surface. *Nano Lett.* **2004**, *4*, 979−983.
(14) Guisinger, N. P.; Greene, M. E.; Basu, R.; Baluch, A. S.; Hersam, M. C. Room Temperature Negative Differential Resistance through Individual Organic Molecules on Silicon Surfaces. *Nano Lett.* **2004**, *4*, 55−59.
(15) Godlewski, S.; Kolmer, M.; Engelund, M.; Kawai, H.; Zuzak, R.; Garcia-Lekue, A.; Saeys, M.; Echavarren, A. M.; Joachim, C.; Sanchez-Portal, D.; et al. Interaction of a conjugated polyaromatic molecule with a single dangling bond quantum dot on a hydrogenated semiconductor. *Phys. Chem. Chem. Phys.* **2016**, *18*, 3854−3861.
(16) Radny, M. W.; Smith, P. V.; Reusch, T. C. G.; Warschkow, O.; Marks, N. A.; Shi, H. Q.; McKenzie, D. R.; Schofield, S. R.; Curson, N. J.; Simmons, M. Y. Single P and As dopants in the Si(001) surface. *J. Chem. Phys.* **2007**, *127*, 184706.
(17) Reusch, T.; Radny, M.; Smith, P.; Warschkow, O.; Marks, N.; Curson, N.; McKenzie, D.; Simmons, M. Single Phosphorus Atoms in Si(001): Doping-Induced Charge Transfer into Isolated Si Dangling Bonds. *J. Phys. Chem. C* **2007**, *111*, 6428−6433.
(18) Scappucci, G.; Capellini, G.; Johnston, B.; Klesse, W. M.; Miwa, J. A.; Simmons, M. Y. A Complete Fabrication Route for Atomic-Scale, Donor-Based Devices in Single-Crystal Germanium. *Nano Lett.* **2011**, *11*, 2272−2279.
(19) Weber, B.; Mahapatra, S.; Ryu, H.; Lee, S.; Fuhrer, A.; Reusch, T. C. G.; Thompson, D. L.; Lee, W. C. T.; Klimeck, G.; Hollenberg, L. C. L.; et al. Ohm's Law Survives to the Atomic Scale. *Science* **2012**, *335*, 64−67.
(20) Kepenekian, M.; Robles, R.; Joachim, C.; Lorente, N. Surface-State Engineering for Interconnects on H-Passivated Si(100). *Nano Lett.* **2013**, *13*, 1192−1195.
(21) Kepenekian, M.; Novaes, F. D.; Robles, R.; Monturet, S.; Kawai, H.; Joachim, C.; Lorente, N. Electron transport through dangling-bond silicon wires on H-passivated Si(100). *J. Phys.: Condens. Matter* **2013**, *25*, 025503.
(22) Robles, R.; Kepenekian, M.; Monturet, S.; Joachim, C.; Lorente, N. Energetics and stability of dangling-bond silicon wires on H passivated Si(100). *J. Phys.: Condens. Matter* **2012**, *24*, 445004.
(23) Kepenekian, M.; Robles, R.; Rurali, R.; Lorente, N. Spin transport in dangling-bond wires on doped H-passivated Si(100). *Nanotechnology* **2014**, *25*, 465703.
(24) Lee, J.; Cho, J.-H.; Zhang, Z. Quantum size effects in competing charge and spin orderings of dangling bond wires on Si(001). *Phys. Rev. B: Condens. Matter Mater. Phys.* **2009**, *80*, 155329.
(25) Raza, H. Theoretical study of isolated dangling bonds, dangling bond wires, and dangling bond clusters on a H:Si(001)-(2 × 1) surface. *Phys. Rev. B: Condens. Matter Mater. Phys.* **2007**, *76*, 045308.
(26) Bellec, A.; Chaput, L.; Dujardin, G.; Riedel, D.; Stauffer, L.; Sonnet, P. Reversible charge storage in a single silicon atom. *Phys. Rev. B: Condens. Matter Mater. Phys.* **2013**, *88*, 241406.
(27) Kawai, H.; Neucheva, O.; Yap, T. L.; Joachim, C.; Saeys, M. Electronic characterization of a single dangling bond on n- and p-type Si(001)-(2 × 1):H. *Surf. Sci.* **2016**, *645*, 88−92.
(28) Bowler, D.; Fisher, A. Small polaron formation in dangling-bond wires on the Si(001) surface. *Phys. Rev. B: Condens. Matter Mater. Phys.* **2000**, *63*, 035310.
(29) Bird, C. F.; Fisher, A. J.; Bowler, D. R. Soliton effects in dangling-bond wires on Si(001). *Phys. Rev. B: Condens. Matter Mater. Phys.* **2003**, *68*, 115318.
(30) Joachim, C.; Renaud, N.; Hliwa, M. The Different Designs of Molecule Logic Gates. *Adv. Mater.* **2012**, *24*, 312−317.
(31) Lorente, N.; Joachim, C., Eds. *Architecture and Design of Molecule Logic Gates and Atom Circuits: Proceedings of the 2nd AtMol. European Workshop*; Advances in Atom and Single Molecule Machines; Springer, 2013.
(32) Dridi, G.; Julien, R.; Hliwa, M.; Joachim, C. The mathematics of a quantum Hamiltonian computing half adder Boolean logic gate. *Nanotechnology* **2015**, *26*, 344003.
(33) Kleshchonok, A.; Gutierrez, R.; Joachim, C.; Cuniberti, G. Quantum interference based Boolean gates in dangling bond loops on Si(100):H surfaces. *Sci. Rep.* **2015**, *5*, 14136.
(34) Lorente, N.; Joachim, C., Eds. *Atomic Scale Interconnection Machines*; Advances in Atom and Single Molecule Machines: Proceedings of the 1st AtMol European Workshop; Springer, 2012.
(35) Kolmer, M.; Zuzak, R.; Dridi, G.; Godlewski, S.; Joachim, C.; Szymonski, M. Realization of a quantum Hamiltonian Boolean logic gate on the Si(001):H surface. *Nanoscale* **2015**, *7*, 12325−30.
(36) Naydenov, B.; Boland, J. J. Engineering the electronic structure of surface dangling bond nanowires of different size and dimensionality. *Nanotechnology* **2013**, *24*, 275202.
(37) Mantega, M.; Rungger, I.; Naydenov, B.; Boland, J. J.; Sanvito, S. Spectroscopic characterization of a single dangling bond on a bare Si(100)-c(4 × 2) surface for n- and p-type doping. *Phys. Rev. B: Condens. Matter Mater. Phys.* **2012**, *86*, 035318.
(38) Peierls, R. E. *Quantum Theory of Solids*; Clarendon: Oxford, 1955.
(39) Mott, N. F. Metal-Insulator Transition. *Rev. Mod. Phys.* **1968**, *40*, 677−683.
(40) Kennedy, T.; Lieb, T. H. No Title. *Phys. Rev. Lett.* **1987**, *59*, 1309−1312.
(41) Grüner, G. The dynamics of charge-density waves. *Rev. Mod. Phys.* **1988**, *60*, 1129.
(42) Wojtaszek, M.; Lis, J.; Zuzak, R.; Such, B.; Szymonski, M. Inversion layer on the Ge(001) surface from the four-probe conductance measurements. *Appl. Phys. Lett.* **2014**, *105*, 042111.
(43) Soler, J. M.; Artacho, E.; Gale, J. D.; García, A.; Junquera, J.; Ordejón, P.; Sánchez-Portal, D. The SIESTA method for ab initio order-N materials simulation. *J. Phys.: Condens. Matter* **2002**, *14*, 2745−2779.
(44) Perdew, J. P.; Burke, K.; Ernzerhof, M. Generalized Gradient Approximation Made Simple. *Phys. Rev. Lett.* **1996**, *77*, 3865.
(45) Labidi, H.; Taucer, M.; Rashidi, M.; Koleini, M.; Livadaru, L.; Pitters, J.; Cloutier, M.; Salomons, M.; Wolkow, R. A. Scanning tunneling spectroscopy reveals a silicon dangling bond charge state transition. *New J. Phys.* **2015**, *17*, 073023.
(46) Koch, W.; Holthausen, M. C. *A chemistas guide to density functional theory*; John Wiley & Sons, Ltd., 2001.
(47) Cohen, A. J.; Tozer, D. J.; Handy, N. C. Evaluation of in density functional theory. *J. Chem. Phys.* **2007**, *126*, 214104.

DOI: 10.1021/acs.jpcc.6b04540
J. Phys. Chem. C 2016, 120, 20303−20309

(48) Huzak, M.; Deleuze, M. S.; Hajgato, B. Half-metallicity and spin-contamination of the electronic ground state of graphene nanoribbons and related systems: An impossible compromise? *J. Chem. Phys.* **2011**, *135*, 104704.
(49) Brandbyge, M.; Mozos, J.-L.; Ordejón, P.; Taylor, J.; Stokbro, K. Density-functional method for nonequilibrium electron transport. *Phys. Rev. B: Condens. Matter Mater. Phys.* **2002**, *65*, 165401.
(50) Lyding, J. W.; Shen, T.-C.; Hubacek, J. S.; Tucker, J. R.; Abeln, G. C. Nanoscale patterning and oxidation of Hpassivated Si(100)2 × 1 surfaces with an ultrahigh vacuum scanning tunneling microscope. *Appl. Phys. Lett.* **1994**, *64*, 2010−2012.
(51) Schofield, S. R.; Curson, N. J.; Simmons, M. Y.; Rueß, F. J.; Hallam, T.; Oberbeck, L.; Clark, R. G. Atomically Precise Placement of Single Dopants in Si. *Phys. Rev. Lett.* **2003**, *91*, 136104.
(52) Ramachandran, P.; Varoquaux, G. Mayavi: 3D Visualization of Scientific Data. *Comput. Sci. Eng.* **2011**, *13*, 40−51.
(53) Hunter, J. D. Matplotlib: A 2D Graphics Environment. *Comput. Sci. Eng.* **2007**, *9*, 90−95.
(54) QuantumWise, Virtual Nanolab.2014.

DOI: 10.1021/acs.jpcc.6b04540
J. Phys. Chem. C 2016, 120, 20303−20309